# Gold Mineralization and Geology in the Zeballos Area, Nootka Sound, Southwestern British Columbia

By Dan Marshall, Scott Close, Natalka Podstawskyj and Adolf Aichmeier

*KEYWORDS:* Zeballos, Nootka, gold veins, fluids, thermobarometry, mineralization, Eocene, sulphur isotopes

## INTRODUCTION

The Zeballos mining camp, located in the Nootka Sound map area (NTS 92E), was an important gold producer in the 1930s and 1940s. Although not the largest gold camp in British Columbia (Schroeter and Pinsent, 2000), it is in all likelihood significantly underexplored due to its poor access, heavy vegetation, mountainous rugged terrain and relative lack of geological research. The region has not been studied in any detail since the regional geological investigations of Muller *et al*. (1981) and, with the exception of two preliminary reports published in the early 1980s (Sinclair and Hansen, 1983; Hansen and Sinclair, 1984), the majority of the geological work on the Zeballos camp was done by Stephenson (1938, 1939, 1950) in the 1930s and 1940s, during the height of mining activity.

A project to investigate the metallogeny of the Zeballos camp and to put the geology and mineral deposits of the area into a modern geological-tectonic context was initiated in August 2004. Work undertaken this summer included:

- regional mapping in the area, including verification of previous work and remapping of Nootka Island in light of our new interpretations of the rock types and tectonic setting of the area;
- sampling of the representative units; intrusive, volcanic, sedimentary and mineralized veins, for lithogeochemistry;
- mapping and sampling underground at the Privateer mine to develop a detailed paragenetic and geochronological framework for gold mineralization at the main producer within the camp; sampling for geochronology included mafic dykes, rhyolite dykes and the Zeballos stock; and
- developing pressure and temperature depositional constraints for gold mineralization at the Privateer mine (as a proxy for the region) from stable isotopes, fluid inclusions and goethermobarometric studies.

## GENERAL GEOLOGY

The Nootka Sound area is underlain by the Wrangellia tectonostratigraphic terrane, which extends from southern Vancouver Island through the Queen Charlotte Islands and into southeastern Alaska and the Yukon. (Jones *et al*., 1977; Wheeler *et al*., 1991). Wrangellia is a large, complex oceanic terrane dominated by extensive accumulations of flood basalt. This terrane was accreted onto the western margin of the North American plate by the Late Jurassic to Early Cretaceous.

The general geology of the study area is complex (*see* Fig. 1, 2) and consists of periods of volcanism punctuated by periods of sedimentation, deformation, metamorphism and hydrothermal activity. The relative timing of volcanism, sedimentation, plutonism, regional fabrics, deformation, metamorphism and mineralization is depicted in Figure 3.

Within the Nootka Sound area around Zeballos and on Nootka Island, the bedrock includes Triassic Karmutsen volcanic rocks and Quatsino limestone (and possibly the Parson Bay formation), collectively known as the Vancouver Group; mid-Jurassic granodiorite, diorite, hornblende diorite and gabbro of the Island Intrusive Suite; and the coeval mid-Jurassic Bonanza volcanic rocks, consisting of andesite pyroclastics and flows, dacite tuffs and flows, and some calcsilicate rocks. All of these rocks are cut by Mount Washington intrusions of the Tertiary Catface intrusive suite. Outcrops of the Carmanah Group conglomerate and sandstone are exposed on the southwest coast of Nootka Island.

The Karmutsen formation is over 3000 m thick and comprises tholeiitic pillow basalt, massive basaltic lavas and comagmatic dykes and sills, with minor sedimentary and volcaniclastic rocks. The origin of the Karmutsen formation is enigmatic but is presently thought to represent oceanic flood basalts associated with a back-arc rift or a primitive marine volcanic arc (Yorath *et al*., 1999). The Quatsino limestone lies conformably on the Karmutsen formation but may be interfolded and interfaulted with the Karmutsen. A gradational contact separates the Quatsino formation from the overlying Parson Bay formation; however, in this study, these two units are mapped together as Quatsino.

The Jurassic calcalkaline rocks of the Bonanza Group unconformably overlie the Triassic rocks of the Vancouver Group. The Bonanza Group is interpreted to be an Early to Middle Jurassic island arc (Debari *et al*., 1999), intruded by the comagmatic Island Intrusive Suite. Emplacement of the Island intrusions at mid-crustal levels produced partial melts and amphibolite-grade metamorphic rocks (Muller *et al*., 1981). These partial-melt metamorphic rocks were

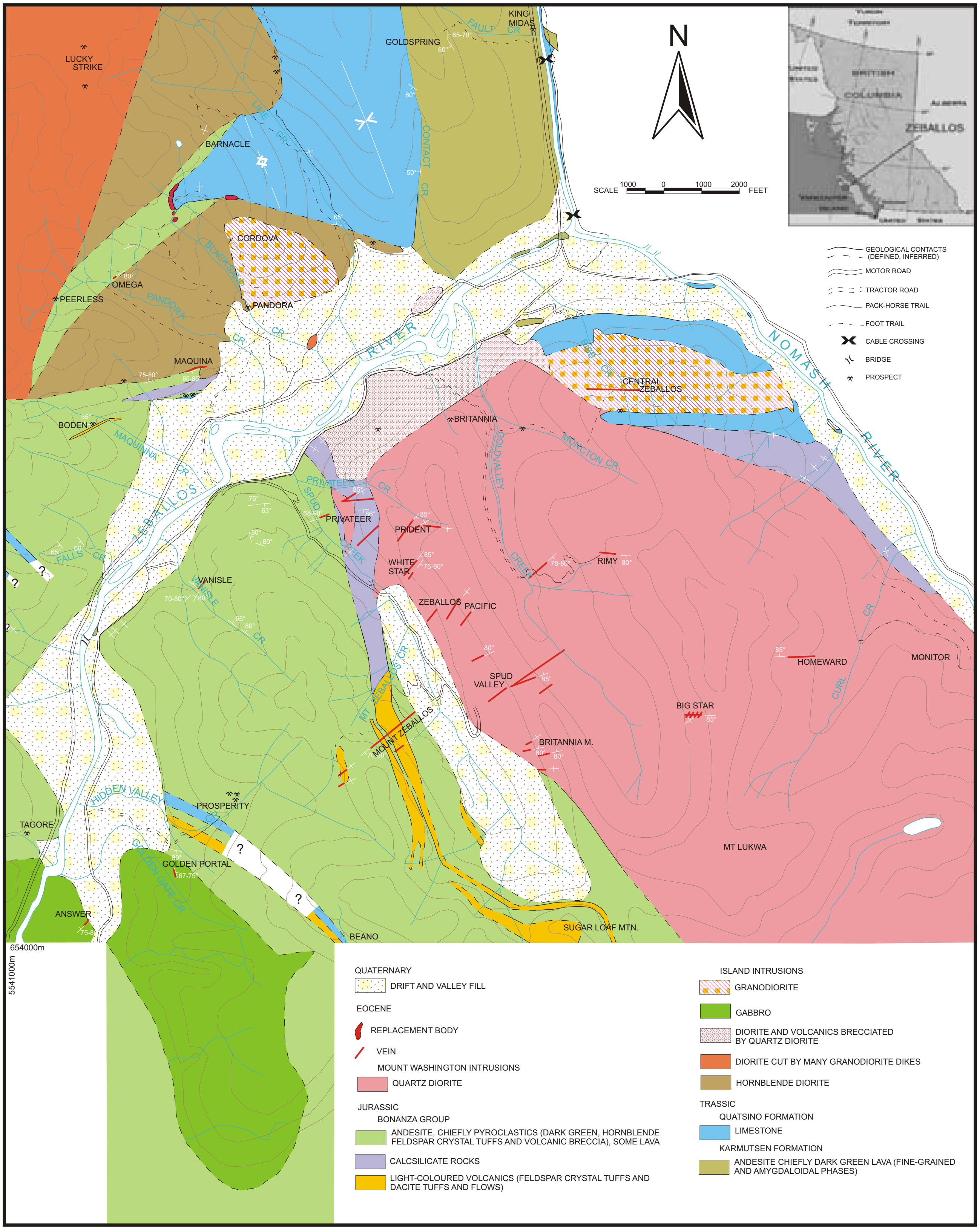

Figure 1. Geology of the Zeballos region (*modified from* Stevenson, 1950).

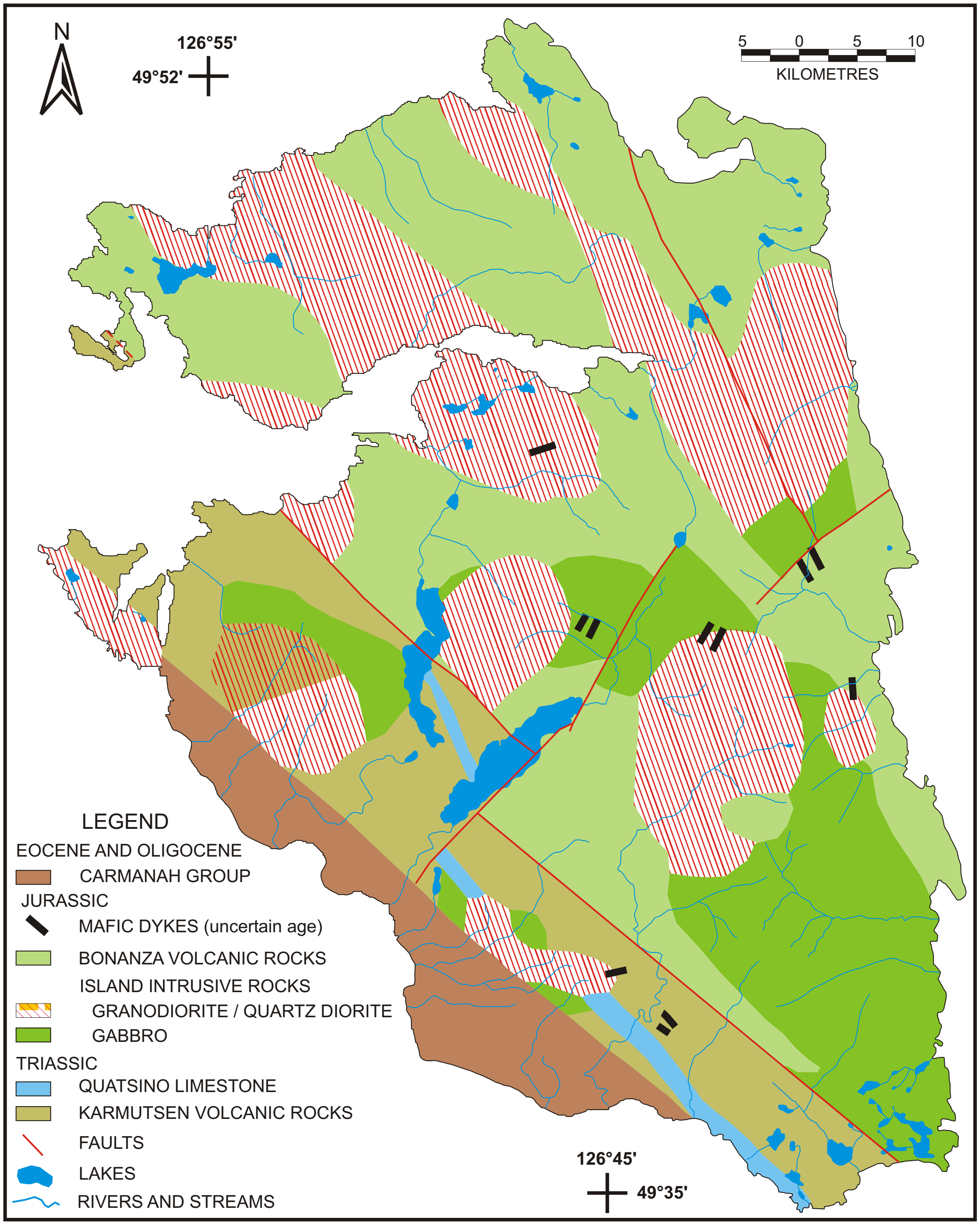

Figure 2. Geology of Nootka Island.

named the Westcoast Crystalline Complex (WCC) by Muller and Carson (1969).

Accretion of Wrangellia to the continental margin occurred between the Late Jurassic and Middle Cretaceous. The Cretaceous Nanaimo Group sediments overlie all the aforementioned rocks just to the east and north of the study area, although there are no outcrops of this formation within the study area.

Tertiary Catface intrusions and succeeding Eocene to Oligocene Carmanah Group sediments are the youngest rocks in the study area. The Carmanah is thought to be age equivalent to the Catface Suite, but contact and timing relationships are still unclear. The Catface intrusions have been subdivided into the older (60–45 Ma) Clayoquot and younger (38–47 Ma) Mount Washington intrusions (Massey, 1995). The Zeballos Stock, which hosts to most of the gold mineralization in the study area, is part of the Mount Washington suite.

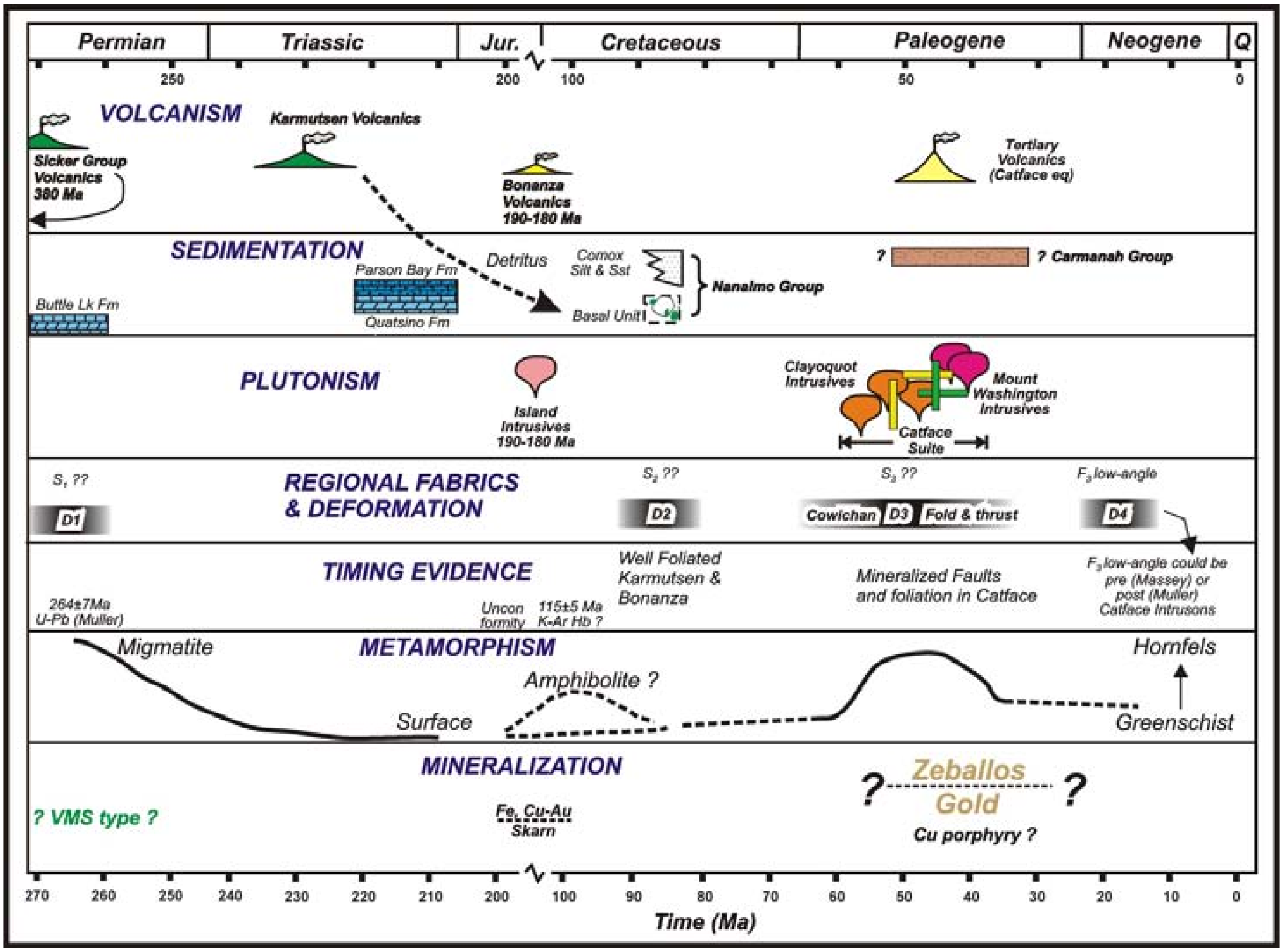

Figure 3. Schematic diagram illustrating the timing of principal geological events in the Nootka Sound region.

## REGIONAL GEOLOGY: REVISIONS TO NOOTKA SOUND MAP UNITS

Large areas of Nootka Island were mapped as the Westcoast Crystalline Complex (WCC) by Muller *et al*. (1981). The WCC was originally identified by Muller and Carson (1969) and described as “a heterogeneous assemblage of amphibolite and basic migmatite with minor metasedimentary and metavolcanic rocks of greenschist metamorphic grade.” It was subsequently subdivided into two mappable units; migmatite and amphibolite, by Muller *et al*. (1981), which they considered to be migmatized preexisting volcanic and sedimentary rocks. Muller *et al*. (1981) suggested that, during Early to Middle Jurassic time, the pre-Jurassic rocks were subjected to very high grade metamorphic conditions, ranging up to migmatitic, and that the highest grade metamorphism yielded the WCC and the Island Intrusive Suite.

Our field observations have not yielded any evidence of an extensive high-grade metamorphic or migmatization event in the area. Rather, exposures of migmatized rock are restricted to what appear to be clasts of country rock stoped into the magma chambers of the Island Intrusive Suite. Metamorphic grade at the time of intrusion of the Island Intrusive Suite appears to have been greenschist.

Mapping and the results from an ongoing geochemical study indicate that the majority of what was mapped as WCC is in fact Island Intrusion, Karmutsen and/or Bonanza volcanic rocks. As the volcanic rocks can generally be identified, we suggest that the Triassic and Jurassic Nootka Island rocks be mapped as meta-Bonanza, meta-Karmutsen or Island Intrusives and thus the term Westcoast Crystalline Complex is superfluous to the list of rock units for Nootka Island (Fig. 2).

The implication of this reinterpretation of the WCC on Nootka Island is two-fold. Firstly, Muller *et al*. (1981) identified extensive areas of WCC elsewhere on the west coast of Vancouver Island and these units should be re-examined. Secondly, the recognition of additional areas of Triassic and Jurassic volcanic and related intrusive rock may increase the prospectivity of parts of the Nootka Sound area for VMS and/or Cu-Ni-PGE mineralization.

## LITHOGEOCHEMISTRY

Thirty-five samples representative of the main rock units in the Zeballos area have been collected for lithogeochemical study. As part of this ongoing geochemical study, these samples will be analyzed for whole-rock major and trace element chemistry and then compared to existing geochemical data sets from similar rocks on Vancouver Island (Massey 1991; 1995; Debari *et al*., 1999; Yorath *et al*., 1999) as an aid to mapping and interpreting tectonic provenance.

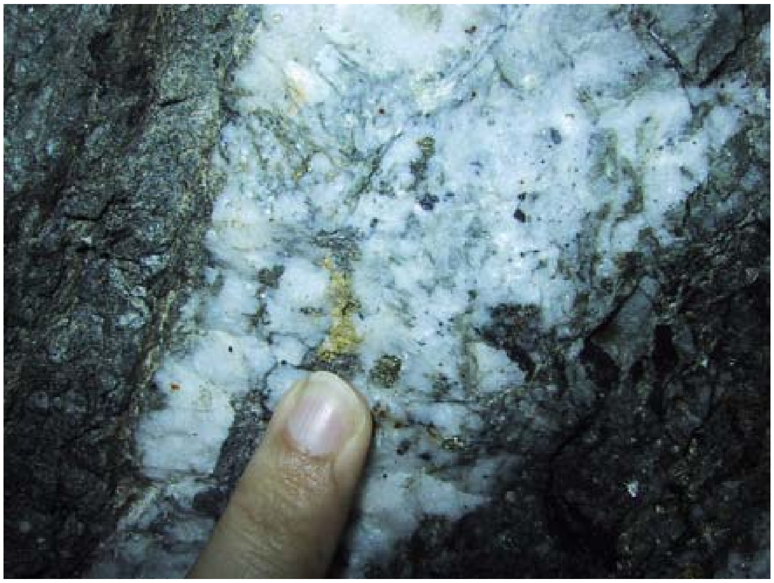

Figure 4. Quartz vein from the Privateer mine. Native gold is visible in association with arsenopyrite at the tip of the finger.

## GOLD VEIN MINERALOGY, PETROGRAPHY AND STRUCTURE (PRIVATEER MINE)

The gold veins at the Privateer mine vary in width up to approximately 30 cm. The veins are hosted within the Zeballos Stock and surrounding calcsilicate (skarn) rocks. The veins comprise, in order of abundance, quartz, calcite, arsenopyrite, pyrite, sphalerite, pyrrhotite, galena, chlorite and gold. The modal mineralogy of the veins is not consistent, but quartz (or quartz-vein breccia fragments) generally constitute some 70% of the vein material. The quartz varies from idiomorphic, clear crystalline quartz displaying cockscomb textures to anhedral, white massive quartz. There is a tendency for the brecciated quartz fragments to have a milky colour. This is probably attributable to the degree of deformation. Euhedral quartz crystals range in size up to 2 cm, while the milky brecciated polycrystalline quartz clasts range up to 10 cm. Calcite and arsenopyrite are generally the second and third most abundant minerals within the veins. Both of these minerals have habits that range from euhedral to anhedral, and grain sizes that vary up to 2 cm. The other vein minerals tend to have smaller grain sizes (rarely achieve sizes of more than a few millimetres) and range from euhedral to anhedral. In some cases, the veins are rich in very fine grained fault gouge, which ranges in colour from silvery-white and grey to dark brown.

Gold concentrations within the veins are sporadic. Visible gold accompanies good gold grades, so a good portion of the gold is deemed to be free gold and not (refractory gold) existing as solid solutions in the arsenopyrite and sulphides. Typical visible gold hosted within an arsenopyrite-rich quartz vein is shown in Figure 4. In more detail (Fig. 5), the timing relationships between gold, arsenopyrite, galena and quartz indicate that quartz is early in the paragenesis, followed by or in some cases contemporaneous with arsenopyrite. Galena replaces arsenopyrite and gold replaces both arsenopyrite and galena. Thus, gold is one of the latest minerals in the paragenetic sequence. Calcite precipitates throughout the paragenesis of the veins, and the other sulphides (pyrite, sphalerite and pyrrhotite) appear to be contemporaneous with galena.

In general, the gold-bearing veins trend northeast and dip steeply. The veins are concentrated on the southwest flank of the Zeballos Stock, suggesting that they formed as

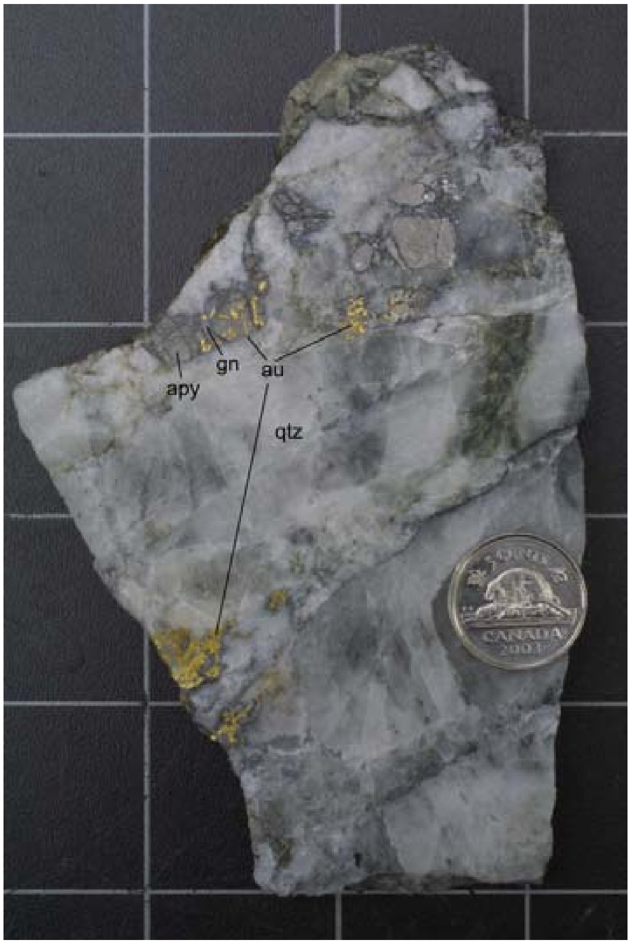

Figure 5. Slab of gold-bearing quartz (qtz) vein from the Privateer mine. Slab length is approximately 15 cm. Note the relationship between the galena (gn), which replaces arsenopyrite (apy), and the gold (au), which cuts both arsenopyrite and galena.

a result of heat from the stock and structures developed during emplacement or related to continuing tectonic forces during cooling. Underground observations at the Privateer mine indicate that the veins formed near the brittle-ductile transition, as both types of structures are observed (Fig. 6) in the veins. The majority of offsets along structures in the mine are sinistral, but there are numerous examples of dextral offsets as well.

Wallrock alteration surrounding the veins is cryptic. In most cases, the granitic wallrock appears to have no alteration halo. Closer inspection reveals that all of the mafic minerals within the Zeballos Stock have been altered to chlorite. The feldspars appear to be unaffected in hand specimen. If the wallrock to the veins is the calcsilicate rocks, there is no wallrock alteration visible. This lack of wallrock alteration is consistent with focused fluid flow along the vein structures and also consistent with the lack of gold or sulphides within the wallrock.

## PRESSURE AND TEMPERATURE CONSTRAINTS ON GOLD MINERALIZATION

### *Fluid Inclusions*

Preliminary fluid inclusion work indicates the presence of at least two fluid inclusion assemblages (FIAs) within the quartz-carbonate gold-bearing veins. Both FIAs occur within the vein carbonate and quartz, but we have limited the microthermometric measurements to inclusions within euhedral quartz crystals (Fig. 7). Both FIAs consist of a liquid and vapour component at room temperature. However, what we interpret to be the early FIA is a $CO_2$-bearing (carbonic) fluid with an aqueous saline liquid, whereas the later FIA consists of only aqueous saline liquid and vapour (i.e., no $CO_2$).

The vapour bubble within the carbonic FIA occupies approximately 20% of the fluid inclusion volume, while the vapour phase in the aqueous inclusions occupies approximately 10% of the inclusion volume. Preliminary petrographic and microthermometric measurements suggest the two FIAs are independent of each other and do not represent conjugates of a boiling system, as both inclusion types homogenize into the liquid phase. Additionally, the smaller bubble size and lower total homogenization temperatures for the aqueous inclusions are consistent with this FIA being later. We interpret this to mean that the carbonic fluid inclusions are responsible for the majority of the minerals precipitated within the gold-bearing quartz-carbonate veins. Moreover, the carbonic fluid inclusions are consistent with the typical gold-bearing quartz veins elsewhere (Ridley and Diamond, 2000).

The microthermometric behaviour of the carbonic inclusions upon cooling from room temperature is as follows. A clathrate phase nucleates at approximately -28°C and continued cooling results in the nucleation of ice at approximately -37°C and the nucleation of solid $CO_2$ at approximately -98°C. Upon heating, the solid $CO_2$ is observed to melt at approximately -58°C. This depression of the freezing point from the triple point of pure CO*2* (at -56.6°C) is due to the presence of some other dissolved gas phase within the vapour phase of the inclusions, most likely $N_2$ or $CH_4$. Continued heating results in ice melting at approximately -4°C, followed by clathrate melting at various temperatures in the +8 to +12°C range. The elevation of the clathrate melting temperature above 10°C is consistent with the dissolved gas being dominantly $CH_4$ rather than $N_2$, but some $N_2$ may also be present. Further heating results in the total homogenization of the fluid inclusion into the liquid phase.

The microthermometric data are consistent with an average fluid composition of $X_{H2O}$ equal to 0.974, an $X_{CO2}$ of 0.020 and $X_{NaCl}$ of 0.006 (2.0 wt % NaCl equivalent). Isochoric data have been derived using the equation of state for $H_2O$-$CO_2$-NaCl of Bowers and Helgeson (1983) and the average composition. The isochores have been used (*see*

Figure 6. Back of the 2-3A vein, Privateer mine. Some deformation is accommodated in a brittle manner, as evidenced by the splays coming off the main vein, while some structures within the vein show ductile deformation textures (*see* arrow). Hammer for scale.

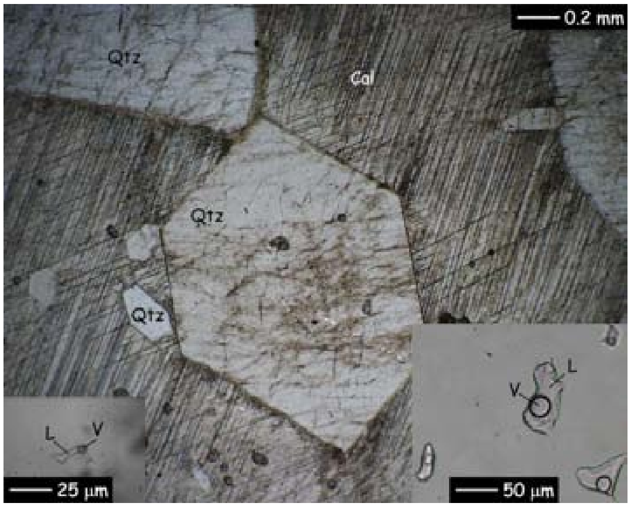

Figure 7. Photomicrograph of euhedral quartz (Qtz) and calcite (Cal) from the gold-bearing quartz-carbonate veins of the Privateer mine. The inset photomicrographs show typical examples of the $CO_2$-bearing fluid inclusions (right) and aqueous fluid inclusions (left). Both FIAs are two-phase inclusions consisting of an aqueous saline liquid (L) and vapour (V). Photos taken in plane polarized transmitted light.

below) to constrain pressure and temperatures of quartz-carbonate vein formation.

### *Sphalerite Geobarometry*

Petrology of the gold-bearing quartz-carbonate veins has shown more paragenetic relationships between sulphides. Most notably, in this case, is sphalerite, pyrite and pyrrhotite in textural equilibrium (Fig. 8). The presence of this assemblage provides the necessary mineralogical constraints to apply the sphalerite geobarometry, as initially developed by Scott and Barnes (1971) and subsequent improvements (Toulmin, 1991 and references within). The sphalerite geobarometer can be used to complement the fluid inclusion work and establish some unique pressure-temperature constraints of vein formation. The sphalerite geobarometer is based on the Fe content of sphalerite in equilibrium with pyrite and pyrrhotite. The electron microprobe analyses of the sphalerite (Fig. 8) are shown in Table 1. The sphalerite Fe compositions were combined with fluid inclusion homogenization temperatures and stable vein assemblages, then plotted on a pressure-temperature diagram (Fig. 9).

### *Sulphur Isotopes*

A sulphur isotope study of coexisting pyrite and sphalerite was carried out to provide an additional constraint on the temperature of vein formation. Sphalerite and pyrite can be seen rimming quartz breccia clasts within vein samples (Fig. 10). Small aliquots of both minerals were extracted from specific locations where there was clear indication of textural equilibrium between sphalerite and pyrite. The sulphur isotope data (Table 2) are consistent with disequilibrium precipitation, using the calibrations of Kajiwara and Krouse (1971) and Ohmoto and Rye (1979). Due to the interpretation of disequilibrium, no temperature data can be derived.

## CONCLUSIONS

The mapping and preliminary lithogeochemistry of Nootka Island indicates the presence of Karmutsen volcanic rocks and Quatsino limestone on the southern portion of the island. These observations and the removal of the West Coast Crystalline Complex from the local stratigraphy means that there is a little more fertile ground for VMS and Ni±PGE mineralization associated with mafic intrusions related to flood basalts, and skarn-type mineralization on Nootka Island. Additionally, these revisions to the bedrock mapping have implications concerning mapping, stratigraphy and tectonic interpretation for the region surrounding Nootka Island.

Preliminary pressure-temperature constraints derived from fluid inclusion studies and combined sphalerite geobarometry of vein material from the Privateer mine are consistent with vein formation temperatures ranging from 300 to 500°C, pressures on the order of 1.5 to 4 kb (Fig. 11) and deposition from a fluid with an average composition of $X_{H2O} = 0.974$, $X_{CO2} = 0.020$ and $X_{NaCl} = 0.006$ (2.0 wt % NaCl equivalent).

## ACKNOWLEDGMENTS

Nick Massey is gratefully acknowledged for many fruitful discussions on the geology, geochemistry and tectonics of the Nootka Sound region. This study was undertaken as part of the Rocks to Riches program, and the authors would like to thank the British Columbia and Yukon Chamber of Mines for partial funding for this study. Additional funding for the study was from an NSERC grant to the senior author and a small grant from NewMex Mining.

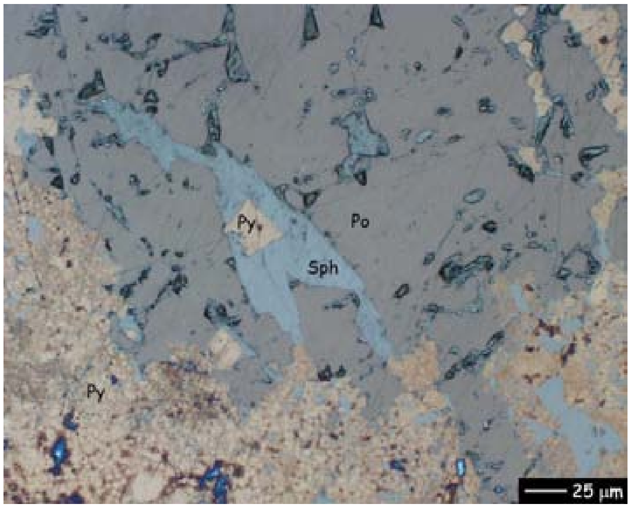

Figure 8. Photomicrograph of intergrown sulphides from the Privateer Mine showing textural equilibrium between pyrite (Py), pyrrhotite (Po) and sphalerite (Sph). Photograph taken in plane polarized reflected light.

TABLE 1. ELECTRON MICROPROBE ANALYSES OF SPHALERITE IN TEXTURAL EQUILIBRIUM WITH PYRITE AND PYRRHOTITE.

| Sample | Zn (wt%) | Fe (wt%) | Mn (wt%) | Cd (wt%) | S (wt%) | Total | Zn (mol) | Fe (mol) | Mn (mol) | Cd (mol) | S (mol) | Total (mol) |
|---|---|---|---|---|---|---|---|---|---|---|---|---|
| ZEB1-C-1 | 57.32 | 8.92 | 0.13 | 0.52 | 33.84 | 100.73 | 0.42 | 0.08 | 0 | 0 | 0.5 | 1 |
| ZEB1-C-2 | 55.97 | 9.77 | 0.15 | 0.54 | 33.82 | 100.25 | 0.41 | 0.08 | 0 | 0 | 0.5 | 1 |
| ZEB1-C-3 | 55.54 | 10.2 | 0.27 | 0.55 | 33.79 | 100.35 | 0.41 | 0.09 | 0 | 0 | 0.5 | 0.999 |
| ZEB1-C-4 | 55.63 | 10 | 0.22 | 0.41 | 33.62 | 99.88 | 0.41 | 0.09 | 0 | 0 | 0.5 | 1.001 |
| ZEB1-C-5 | 55.05 | 10.41 | 0.25 | 0.54 | 33.95 | 100.2 | 0.4 | 0.09 | 0 | 0 | 0.51 | 1 |
| ZEB1-B16 | 57.13 | 8.82 | 0.17 | 0.57 | 32.87 | 99.56 | 0.42 | 0.08 | 0 | 0 | 0.5 | 0.999 |
| ZEB1-B17 | 55.99 | 8.99 | 0.15 | 0.54 | 33.42 | 99.09 | 0.41 | 0.08 | 0 | 0 | 0.5 | 0.999 |
| ZEB1-B18 | 56.1 | 9.91 | 0.18 | 0.6 | 33.51 | 100.3 | 0.41 | 0.09 | 0 | 0 | 0.5 | 1.001 |
| ZEB1-B19 | 56.53 | 10.23 | 0.21 | 0.57 | 33.37 | 100.91 | 0.41 | 0.09 | 0 | 0 | 0.5 | 0.999 |
| ZEB1-B20 | 56.46 | 10.63 | 0.21 | 0.58 | 33.5 | 101.38 | 0.41 | 0.09 | 0 | 0 | 0.5 | 1 |
| ZEB1-B21 | 53.94 | 10.59 | 0.22 | 0.55 | 33.79 | 99.09 | 0.4 | 0.09 | 0 | 0 | 0.51 | 0.999 |
| ZEB1-B22 | 56.36 | 10.48 | 0.22 | 0.51 | 33.59 | 101.16 | 0.41 | 0.09 | 0 | 0 | 0.5 | 0.999 |
| ZEB1-B23 | 56.44 | 10.22 | 0.16 | 0.66 | 33.78 | 101.26 | 0.41 | 0.09 | 0 | 0 | 0.5 | 1 |
| ZEB1-B24 | 57.4 | 9.72 | 0.11 | 0.56 | 33.56 | 101.35 | 0.42 | 0.08 | 0 | 0 | 0.5 | 1 |
| ZEB1-B25 | 56 | 9.07 | 0.1 | 0.53 | 32.81 | 98.51 | 0.42 | 0.08 | 0 | 0 | 0.5 | 0.999 |

Abbreviations: wt%, weight percent; mol, molecular proportion.

Support of the local road builders, forestry workers and residents of the area is greatly appreciated. Their interest in basic prospecting and their generous provision of logistical assistance was of significant benefit to this study.

## REFERENCES

Bowers, T.S. and Helgeson, H.C. (1983): Calculation of the thermodynamic and geochemical consequences of nonideal mixing in the system $H_2O$-$CO_2$-NaCl on phase relations in geologic systems: equation of state for $H_2O$-$CO_2$-NaCl fluids at high pressures and temperatures; *Geochimica Cosmochimica Acta*, Volume 47, pages 1247–1275.

DeBari, S.M., Anderson, R.G. and Mortensen, J.K. (1999): Correlation among lower to upper crustal components in an island arc: the Jurassic Bonanza arc, Vancouver Island, Canada; *Canadian Journal of Earth Sciences*, Volume 36, pages 1371–1413.

Hansen, M.C. and Sinclair, A.J. (1984): A preliminary assessment of Zeballos mining camp (92L); *in* Geological Fieldwork, 1983, *BC Ministry of Energy, Mines and Petroleum Resources*, pages 219–232.

Jones, D.L., Silberling, N.J. and Hillhouse, J. (1977): Wrangellia – a displaced terrane in northwestern North America; *Canadian Journal of Earth Sciences*, Volume 14, pages 2565–2577.

Kajiwara, Y. and Krouse, H.R. (1971): Sulphur isotope partitioning in the metallic sulfide systems; *Canadian Journal of Earth Sciences*, Volume 8, pages 1397–1408.

Massey, N.W.D. (1991): The geology of the Port Alberni – Nanaimo Lakes area: *BC Ministry of Energy, Mines and Petroleum Resources*, Geoscience Map 1991-1.

Massey, N.W.D. (1995): Geology and mineral resources of the Alberni – Nanaimo Lakes sheet, Vancouver Island, 92 F/1W, 92 F/2E and part of 92 F/7E; *BC Ministry of Energy, Mines and Petroleum Resources*, Paper 1992-2, 132 pages.

Muller, J.E. and Carson, D.J. (1969): Geology and mineral deposits of Alberni map-area, British Columbia, (92F); *Geological Survey of Canada*, Paper 68-50, 52 pages.

Ohmoto, H. and Rye, R.O. (1979): Isotopes of sulfur and carbon; *in* Geochemistry of Hydrothermal Ore Deposits (2nd edition, Barnes, H.L., Editor, John Wiley and Sons, New York, pages 509–567.

Ridley, J.R. and Diamond, L.W (2000): Fluid chemistry of orogenic lode gold deposits and implications for genetic models; *in* Gold in 2000, Hagemann S. and Brown, P., Editors, *Reviews in Economic Geology*, Volume 13, pages 141–162.

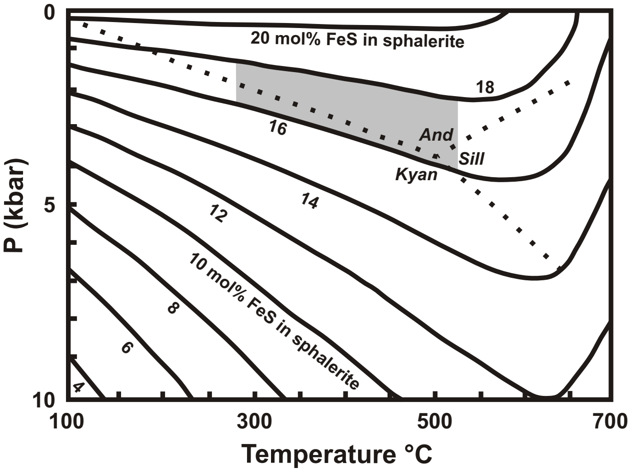

Figure 9. Sphalerite geobarometry diagram showing the isocompositional contours for mole % FeS for sphalerite in equilibrium with pyrite and pyrrhotite (Toulmin, 1991). The position of the aluminosilicate triple point is shown for reference in a dashed pattern. The range of compositions reported from electron microprobe analyses is shown in grey, with the lower temperature constraint defined by fluid inclusion total homogenization temperatures and the upper temperature constraint based on stable mineral assemblage within the veins. Abbreviations: And, andalusite; Kyan, kyanite; Sill, sillimanite.

Schroeter, T. and Pinsent, R.H. (2000): Gold production and resources in BC (1858–1998); *BC Ministry of Energy and Mines*, Open File 2000-2.

Scott, S.D. and Barnes, H.J. (1971): Sphalerite geothermometry and geobarometry; *Economic Geology*, Volume 66, pages 653–669.

Sinclair, A.J. and Hansen, M.C. (1983): Resource assessment of gold-quartz veins, Zeballos mining camp, Vancouver Island: a preliminary report (92L); *in* Geological Fieldwork 1982, *BC Ministry of Energy, Mines and Petroleum Resources*, pages 290–303.

Stephenson, J.S. (1938): Lode-gold deposits of the Zeballos area, west coast of Vancouver Island, British Columbia; *BC Department of Mines*, Bulletin 20.

Stephenson, J.S. (1939): Geology and ore deposits of the Zeballos area, British Columbia; *Transactions of the Canadian Institute of Mining and Metallurgy and of the Mining Society of Nova Scotia*, Volume 42.

Stephenson, J.S. (1950): Geology and mineral deposits of the Zeballos mining camp; *BC Department of Mines*, Bulletin 27, 145 pages.

Toulmin, P. (1991): Commentary on the sphalerite geobarometer; *American Mineralogist*, Volume 76, Numbers 5–6, pages 1038–1051

Wheeler, J.O., Brookfield, A.J., Gabrielese, H., Monger, J.W.H., Tipper, H.W. and Woodsworth, G.J. (1991): Terrane map of the Canadian Cordillera; *Geological Survey of Canada*, Map 1713.

Yorath, C.J., Sutherland Brown, A. and Massey, N.W.D. (1999): Lithoprobe, Southern Vancouver Island, British Columbia: geology; *Geological Survey of Canada*, Bulletin 498, 145 pages.

Figure 10. Slab of quartz carbonate vein containing brecciated vein material rimmed by sphalerite (Sph) and pyrite (Py). The circles indicate the areas where coexisting pyrite and sphalerite were sampled for sulphur isotopes. Pen for scale.

**TABLE 2. SULPHUR ISOTOPE DATA FROM PYRITE-SPHALERITE MINERAL PAIRS.**

| Sample | Mineral | $\delta^{34}S_{CDT}$ | $\Delta^{34}S_{py\text{-}sph}$ | Temperature[1] (°C) |
|---|---|---|---|---|
| 04-666-01 | pyrite | -0.5 | -1 | disequilibrium |
| 04-66601 | sphalerite | 0.5 | | |
| 04-66602 | pyrite | 0.3 | -0.6 | disequilibrium |
| 04-66602 | sphalerite | 0.9 | | |
| 04-66603 | pyrite | -0.3 | -0.3 | disequilibrium |
| 04-66603 | sphalerite | 0 | | |

[1] Temperatures calculated using calibration of Kajiwara and Krouse (1971)

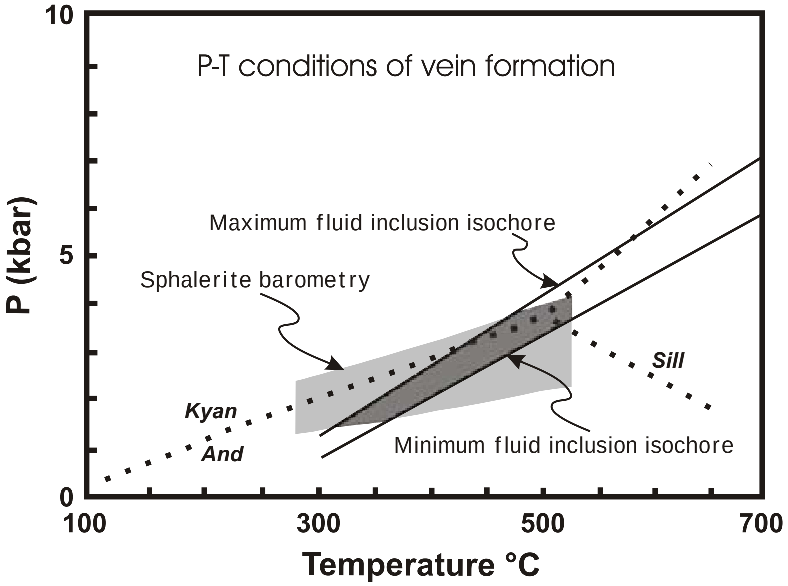

Figure 11. Pressure temperature diagram showing the range of conditions for quartz-carbonate vein formation (dark grey) from the combined constraints of sphalerite geobarometry and the fluid inclusion isochores.